### Title

Applied electric fields polarize initiation and growth of endothelial sprouts.

#### **Authors**

Anyesha Sarkar<sup>1</sup>, Shanta M. Messerli<sup>2,3</sup>, Md Moin Uddin Talukder<sup>1</sup>, and Mark A. Messerli<sup>1\*</sup>

- <sup>1</sup> Department of Biology and Microbiology, South Dakota State University, Brookings, SD, 57007
- <sup>2</sup> Sanford Research, Sioux Falls, SD 57104, USA
- <sup>3</sup> Department of Biomedical Engineering, University of South Dakota, Sioux Falls, SD 57107 USA

## **Abstract**

Therapeutic electric fields (EFs) are applied to the epidermis to accelerate healing of chronic epidermal wounds and promote skin transplantation. While research has emphasized understanding the role of EFs in polarizing the migration of superficial epidermal cells, there are no reports describing the effect of EFs on polarization of the underlying vasculature. We explored the effects of EFs on the growth of endothelial sprouts, precursors to functional blood vessels. We discovered that DC EFs of the same magnitude near wounded epidermis, polarize initiation, growth, and turning of endothelial sprouts toward the anode. While EFs polarize sprouts they do not change the frequency of primary sprout or branch formation. Unidirectional electrical pulses also polarize sprouts based on their time-averaged, EF magnitude. Sprout polarization occurs antiparallel to the direction of electrically-driven water flow (electro-osmosis) and is consistent with the direction of sprout polarization induced by pressure-driven flow. These results support the role of EFs for controlling the direction of neovascularization during healing of soft tissues and tissue engineering.

Keywords: endothelial sprout, electric fields, polarized growth, electro-osmosis, electrokinetic perfusion

Running title: electric fields polarize sprout growth

\* author for correspondence. Mark.Messerli@sdstate.edu

ORCID 0000-0002-0629-9168

Anyesha Sarkar anyeshas1992@gmail.com

Md Moin Uddin Talukder mdmoinuddin.talukder@jacks.sdstate.edu Shanta M. Messerli Shanta.Messerli@sanfordhealth.org

ORCID 0000-0003-3221-0486

### **Author Contributions**

MM and SM originated the ideas and experimental plan. AS, MT and MM performed experiments and analyzed results. All authors were involved with writing and editing the manuscript.

### Introduction

Mass transfer through the cardiovascular system is required for cell function and survival in most tissues and organs. Therefore, rebuilding of the vasculature through neovascularization is required for successful tissue repair, reconstruction, and replacement<sup>(1, 2)</sup>. Neovascularization involves formation of endothelial sprouts, precursors to mature blood vessels<sup>(3)</sup>. Endothelial cell migration and sprout growth are guided into the necessary regions of tissues and organs through a combination of chemotactic, haptotactic, and mechanotactic cues<sup>(4, 5)</sup>. Controlling the growth direction of endothelial sprouts would be most useful to promote *in vivo* tissue repair and construction of vascularized replacement tissues and organs.

We tested the hypothesis that sprout growth may be polarized by electrical cues. *In vitro*, applied electric fields (EFs) below the sensory threshold of electrically excitable cells, polarize cells and direct their migration (galvanotaxis) and growth (galvanotropism)<sup>(6-8)</sup>. It has been proposed that applied EFs polarize cells by concentrating cell surface receptors toward one of the electrical poles<sup>(9, 10)</sup>. However, EFs also promote electrokinetic perfusion, i.e. electrically driven water flow (electro-osmosis) in the interstitial space<sup>(11, 12)</sup> and could generate mechanical signals that polarize cells.

In vitro, EFs polarize and direct migration of endothelial progenitor cells and endothelial cells toward one of the electrical poles<sup>(13-15)</sup>. In vivo, electrical stimulation enhances growth of the local vasculature<sup>(16, 17)</sup>. However, nothing is reported about the electrical sensitivity of the direction of endothelial sprout growth. In vitro, endothelial sprouts develop from sheets or clusters of endothelial cells<sup>(18, 19)</sup>. Here, we report our discovery that EFs polarize the initiation, growth, and turning of human umbilical vein endothelial cell (HUVEC) sprouts toward the anode, the opposite direction of migration of individual HUVECs under similar conditions. We explore DC, pulsed, and alternating EFs to test the mechanisms by which the non-excitable sprouts sense EFs. We also provide <u>in vitro</u> evidence that transepidermal electrical stimulation could promote sprout polarization *in vivo*.

### **Materials and Methods**

Studies of endothelial sprout growth in fibrin gels were performed using cultures of endothelial sheets on Cytodex 3 microcarrier beads (Sigma-Aldrich, St. Louis, MO) and cultures of endothelial cell clusters. HUVECs (Lonza, Walkersville, MD) were cultured in EGM-2 media consisting of EBM-2 basal media with EGM-2 singlequot supplements according to manufacturer's instructions (Lonza, Walkersville, MD). HUVEC structures were grown in coculture with skin fibroblasts in fibrin gels to promote sprout formation and exposed to EFs of 50, 155, and 360 mV/mm in IBIDI channel slides as previously described<sup>(11)</sup>. The experimental arrangements of the IBIDI channels is illustrated in Fig. 1. Phase contrast images of sprouts

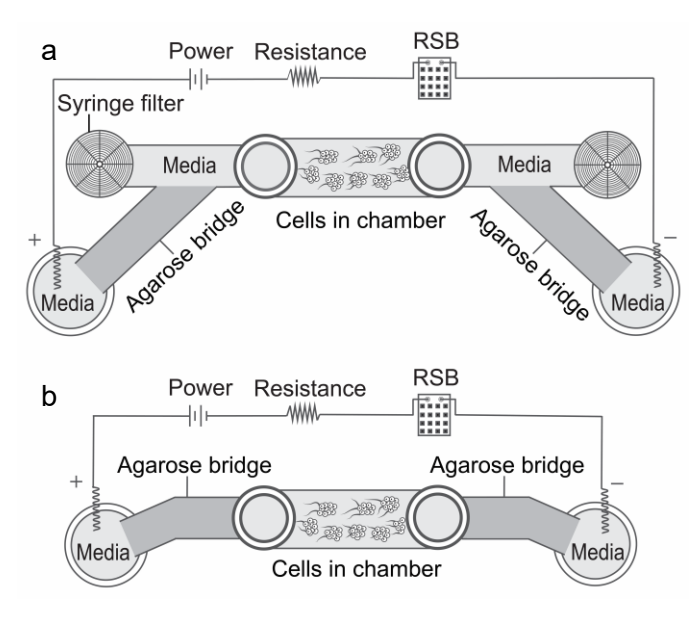


Figure 1. Experimental channel design. EFs were applied to HUVEC structures in IBIDI channel slides. A series resistor and resistance substitution box (RSB) were used to monitor and control the electric field in the channels. a. The open channel design enabled easier exchange of media by simply removing the syringe filters. This design also provided a low resistance pathway for fluid flow from the anode to the cathode side of the channel. **b**. The closed channel design involved directly connecting the low electroendoosmosis (EEO) agarose bridges to the IBIDI wells. While cathodedirected electro-osmotic flow (EOF) continues along negatively charged surfaces through the channel, fluid pressure gradients dissipate in the reverse direction through the porous fibrin matrix.

grown in the absence or presence of EFs were collected after 48 hr. Considering the density and growth rate of cultured sprouts, 48 hrs. allowed substantial growth without excessive overlap or anastomosis that would have made sprout analysis more difficult. Sprouts and their branches were traced using the line segment tool in ImageJ and the line segments were analyzed using Matlab scripts (MathWorks, Natick MA). Further details of the experimental procedures, sprout analysis, and electrokinetic perfusion measurements are provided in the Appendix.

### **Statistical Analysis**

The statistical significance of polarized sprout initiation, growth, and turning was determined using one-tailed t-tests. Statistical significance between other results were compared using one-tailed or two-tailed t-tests as listed in the text.

### Results

In the absence of fibroblasts, sheets and clusters of HUVECs dissociate in fibrin gels containing EGM-2 media, Fig. 2a-b. Under those conditions, individual HUVECs migrate toward the cathode (negative pole) in DC EFs, Fig. 2c-d, similar to their migration direction in 2D culture, Fig. 3. HUVEC sheets on the large Cytodex beads were considered to distort the local EF so most experimentation with sprout polarization occurred with the smaller HUVEC clusters.

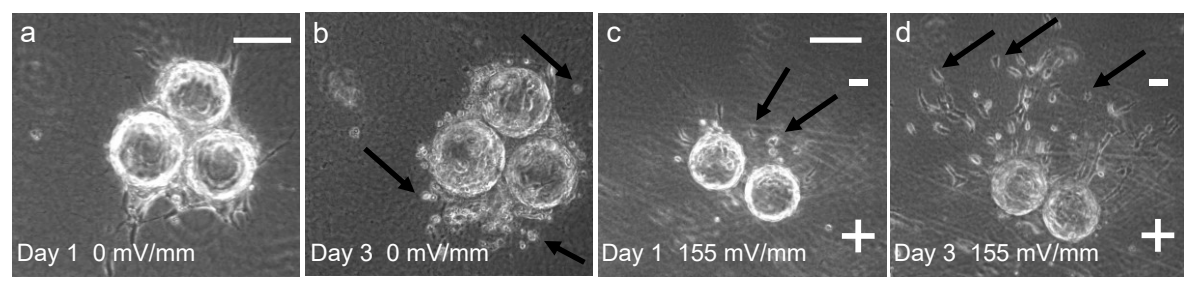


**Figure 2**. **Photos of endothelial cell migration in fibrin gels in the absence of fibroblasts. a.** After one day in fibrin gel, the endothelial cells remained tightly adhered to the collagen coated beads and small sprouts formed. **b.** After three days in the absence of fibroblasts, endothelial cells had detached from the beads and migrated into the fibrin gel (black arrows). **c.** In the presence of a 155 mV/mm DC EF some cells started migrating toward the cathode in the fibrin gel (black arrows) after one day. **d.** After 3 days in the EF, many of the cells had detached from the beads and migrated toward the cathode pole in the fibrin gel (black arrows) at significantly greater distances than in the absence of the EF shown in Fig. 2b. (scale bars 100 μm)

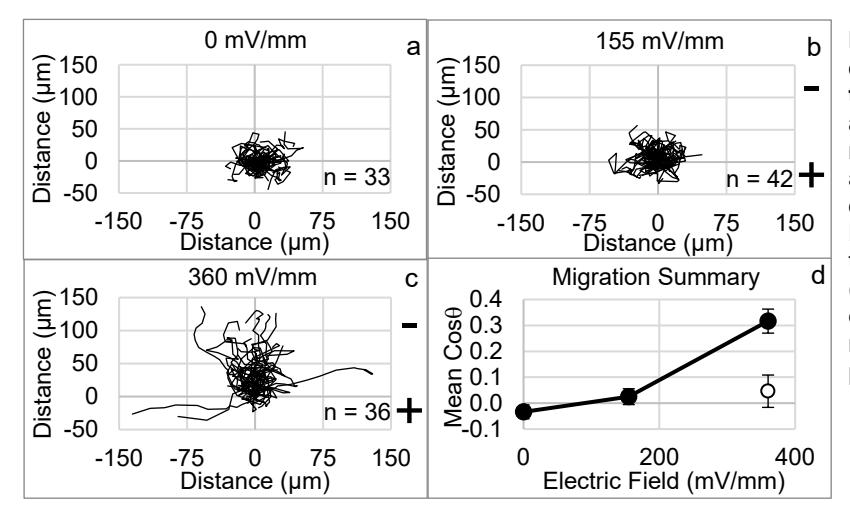
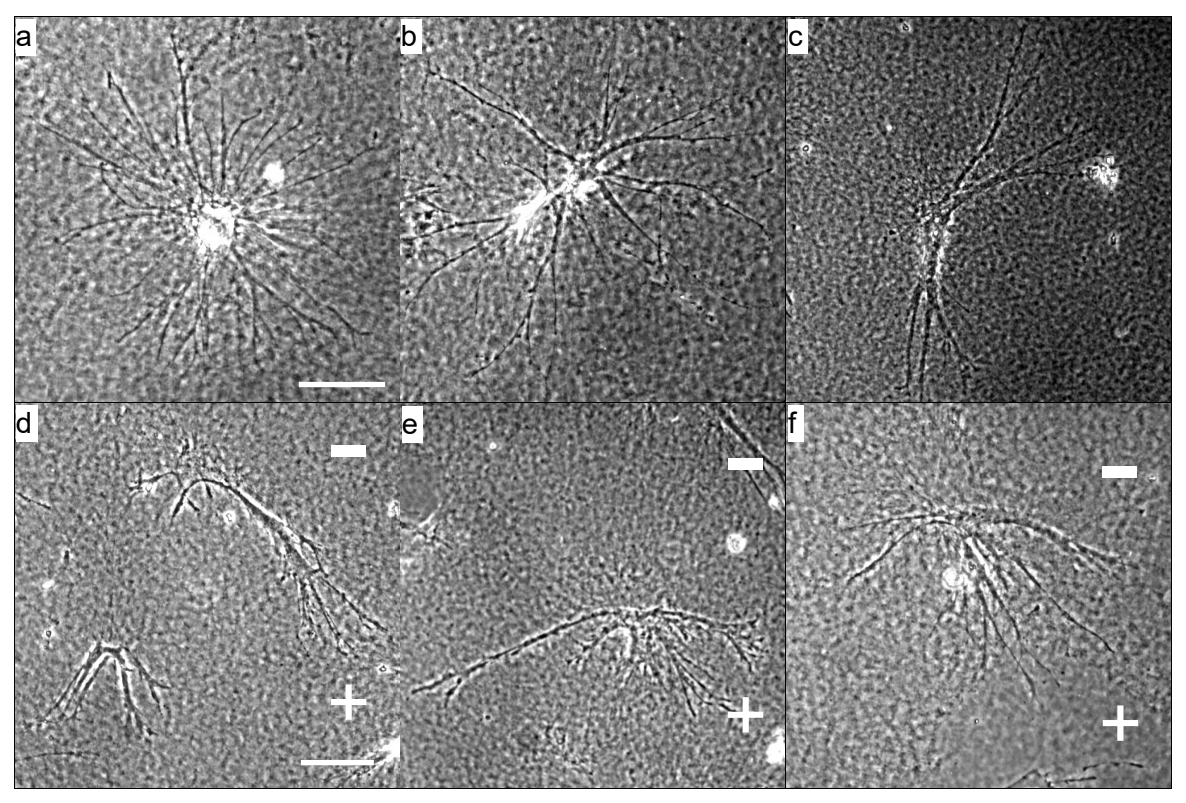


Figure 3. EFs direct single endothelial cell migration toward the cathode.

**a-c.** Trajectory plots for single migrating HUVECs in the absence and presence of applied DC EFs over a period of 4 hours. **d**. HUVECs cultured on glass migrate toward the cathode in an applied EF (●), cathode is positive. When exposed to 360 mV/mm HUVECs migrate randomly on tissue culture plastic (○) (n=11).

In co-culture with skin fibroblasts, HUVEC clusters remain stationary and initiate sprouts that grow persistently away from the HUVEC mass, Fig. 4a-c. Fibroblasts provide a number of factors that promote sprout formation in the absence of EFs (20) and are expected to be necessary in the presence of EFs. Sprouts and their branches were traced for further analysis, Fig 5a1-e1. In the presence of EFs, cell sheets on collagen coated beads remain stationary and display sprout growth toward the anode, indicating that no movement of the central cell mass is required for the asymmetry in sprout growth. In the absence of EFs, the asymmetry between vertical and

horizontal growing sprouts, Fig. 5a1-a2, reflects the long (17 mm) and short (3.8 mm) axes of the IBIDI culture channels, respectively, and the fact that sprouts that grew against the channel side walls were not quantitated. Therefore, growth of EF-exposed sprouts was compared to growth of sprouts in the absence of EFs for simultaneous cultures.



**Figure 4**. **Photos of endothelial sprouts**. **a-c** Sprouts grow persistently away from the cell mass in the absence of applied EFs. **d-f** Sprouts grow toward the anode in the presence of DC EFs of 360 mV/mm. (scale bars  $100 \mu m$ )

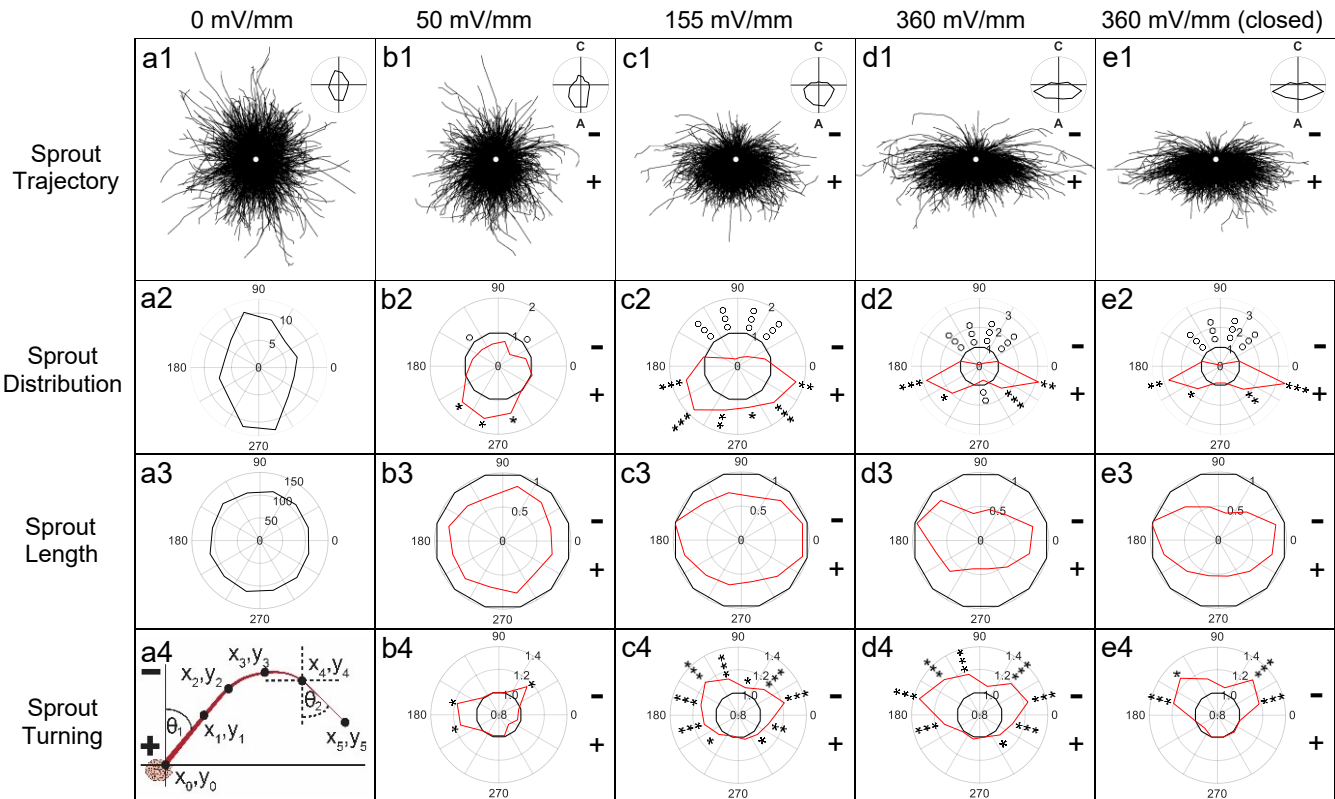


Figure 5. DC EFs polarize endothelial sprouts. a1-e1. Superimposed sprout tracings display increasing anodal polarization with EF strength. (origin = white disk) Insets display the relative distribution of all sprouts for each 30° region of each condition, C-cathode, A-anode. a2. Regional comparison of relative sprout distribution in the absence of EFs (100 • Σ sprout length per region / Σ sprout length for all regions). b2-e2. Relative distribution of EF-exposed sprouts (red) normalized to the relative sprout distribution determined in the absence of EFs (black) for each condition. a3. Average sprout length (μm) remains the same for all regions in the absence of EFs. b3-e3. EFs decrease average relative sprout length (red) compared to sprouts grown simultaneously in the absence of EFs (black). a4. Sprouts were traced using the line segment tool in ImageJ and used to determine the  $\Delta$ cosθ values between the initial segment (θ<sub>1</sub>), and the final segment (θ<sub>2</sub>) of each sprout. b4-e4. Relative average turning of EF-exposed sprouts (red) normalized to sprout turning determined in the absence of EFs (black). Cathodal turning (<1), no net turning (=1), anodal turning (>1). One-tailed t-tests were used to assess statistical significance for increased (\*) or decreased (°) growth or turning. (one symbol, 0.002 < p < 0.02, two symbols, 0.0002 < p < 0.002, three symbols, p < 0.0002)

### **Sprout Initiation**

Sprout growth is polarized toward the anode (positive pole) at 50 mV/mm and increases with field strength, Figs. 4d-f, 5b1-d1. The relative distribution of EF-exposed sprouts, Fig. 5b2-d2 (red), indicates significantly greater anodal growth and lesser cathodal growth compared to sprouts grown in the absence of EFs (black). EFs did not significantly alter the average number of primary sprouts per channel, Table 1.

Table 1 Summary of primary sprout number.

Average Field	Primary sprout
Strength (mV/mm)	number per channel
	(mean ± s.d.)
DC control 0	629 ± 271 (n = 16)
DC 50	912 ± 291 (n=3) <sup>†</sup>
DC 155	536 ± 270 (n=10) <sup>†††</sup>
DC 360	819 ± 592 (n=6) <sup>†††</sup>
(open channels)	
DC 360	706 ± 234 (n=4)†††
(closed channels)	
alternating control 0	750 ± 85 (n = 3)
alternating (±360) 0	844 ± 53 (n = 3) <sup>††</sup>
pulsed control 0	959 ± 111 (n = 6)
pulsed 51.4	1206 ± 548 (n = 3) <sup>††</sup>
pulsed 180	1154 ± 115 (n = 3)†††
$(t_n > 0.05, t_{n>0.1}, t_{n>0.5})$	

 $(^{\dagger}p > 0.05, ^{\dagger\dagger}p > 0.1, ^{\dagger\dagger\dagger}p > 0.5)$ 

Increased anodal growth is accompanied by polarization of primary sprout initiation, Fig. 6. In the absence of EFs, sprout initiation is evenly distributed across the x-axis, with a relative initiation direction close to zero,  $0.03 \pm 0.02$ . In the presence of EFs, the direction of initiation (( $\Sigma$  number of anode initiating sprouts –  $\Sigma$  number of cathode initiating sprouts) /  $\Sigma$  total number of sprouts) is significantly polarized toward the anode at 50 mV/mm,  $0.31 \pm 0.03$  (p < 0.002 one-tailed t-test) and increases to  $0.54 \pm 0.03$  and  $0.63 \pm 0.04$  at 155 and 360 mV/mm, respectively.

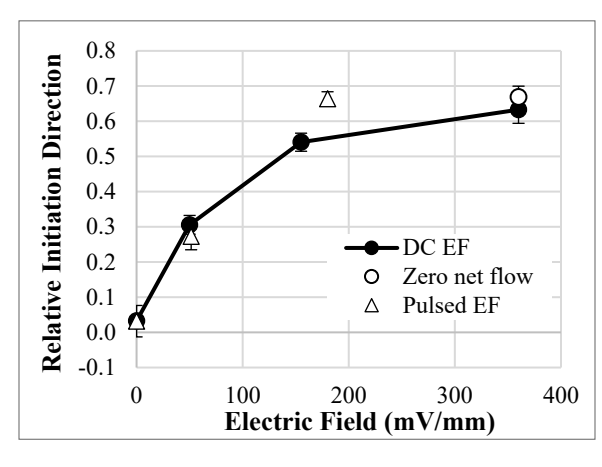


Figure 6. EFs direct sprout initiation toward the anode. (●) DC EFs significantly polarize sprout initiation toward the anode at 50 mV/mm and increase anodal initiation at 155 and 360 mV/mm. (○) Polarized initiation toward the anode at 360 mV/mm in the closed channels, where there is no net fluid flow, is not statistically different than initiation in the open channels at the same field strength (p > 0.5). (△) Pulsed EFs of 360 mV/mm with alternating direction, possessing a time-averaged EF of 0 mV/mm, showed no difference in direction of initiation. Unidirectional pulsed EFs of 360 mV/mm with 14.3% and 50% duty cycles with time-averaged EFs of 51.4 and 180 mV/mm, respectively, significantly polarize sprout initiation toward the anode (p < 0.01 and p < 0.0001).

## **Sprout Growth**

EFs direct greater relative growth of sprouts and their branches toward the anode and away from the cathode, Fig. 5b2-d2. On average,  $25.9 \pm 5.3\%$  of primary sprouts had branches in the absence of EFs, with no consistent increase in the number of branches in the presence of EFs, (p > 0.1 for 50 mV/mm (28.1  $\pm$  4.6%) and 360 mV/mm (35.3  $\pm$  4.1%), p < 0.02 for 155 mV/mm (36.4  $\pm$  11.3%) two-tailed t-test). In the absence of EFs, the relative initiation direction for branches is 0.10  $\pm$  0.12. EFs significantly polarize branch initiation toward the anode, i.e. 0.53  $\pm$  0.14 at 50 mV/mm (p < 0.005), and 0.65  $\pm$  0.05 and 0.67  $\pm$  0.07 at 155 and 360 mV/mm, respectively (p < 10<sup>-5</sup> for both conditions).

Exposure to 50 mV/mm significantly reduced relative growth toward the cathode at  $30-60^{\circ}$  and  $120-150^{\circ}$  and increased relative sprout growth toward the anode at  $210-300^{\circ}$ , Fig. 5b2. On average, larger EFs decreased relative cathodal growth of cathode initiating sprouts at  $30-150^{\circ}$  and increased relative anodal growth of anode initiating sprouts at  $180-360^{\circ}$ , Fig. 5c2-d2. At 155 and 360 mV/mm, relative lateral-anodal sprout growth at  $180-240^{\circ}$  and  $300-360^{\circ}$  is significantly greater than growth directly facing the anode at  $240-300^{\circ}$  (p <  $10^{-3}$  for both conditions).

While anodal polarization increases, average sprout length decreases with increasing field strength. Average sprout length after 48 hrs. in the absence of EFs is 112.0  $\pm$  2.4  $\mu$ m, ranging between 108.3 – 115.8  $\mu$ m for each of the 12 polar regions. When exposed to 50, 155, and 360

mV/mm, average sprout length decreased to  $0.75\pm0.05$  (range 0.67-0.83),  $0.79\pm0.12$  (range 0.63-1.01), and  $0.62\pm0.18$  (range 0.41-0.97) (mean  $\pm$  s.d.) of sprouts grown in the absence of EFs, respectively, Fig. 5b3-d3. In EFs of 155 and 360 mV/mm, sprout length parallel to the EFs (60-120° and 240-300°) is reduced to 0.67 and 0.44 of sprout length in the absence of EFs, significantly lower than 0.93 and 0.79 (p <  $10^{-8}$  for both comparisons, one-tailed t-test), the average relative sprout lengths perpendicular to the EFs (330-30° and 150-210°).

## **Sprout Turning**

EFs also enhance turning of primary sprouts toward the anode. Average turning was assessed by calculating the average  $\Delta\cos\theta$  between the initial and final line segments used to trace each primary sprout, illustrated in Fig. 5a4. Each region of the polar plots in Fig. 5b4-5d4, indicates the average  $\Delta\cos\theta$  for the sprouts that initiated in that region. In the absence of EFs, the average  $\Delta\cos\theta$  for the 12 different regions is  $1.01\pm0.06$ , indicating no net turning trend. Exposure to 50 mV/mm, Fig. 5b4, significantly increases turning of sprouts toward the anode at 30-60° and 150-210°. In the presence of 155 and 360 mV/mm, Fig. 5c4-d4, anodal turning increases for most of the regions outside 240-300°. Sprouts that initiate toward the anode, 240-300°, grow persistently toward the anode. Sprouts that initiate at angles perpendicular to the EF or toward the cathode, show greater average turning away from the cathode.

# **Role of Extracellular Water Flow**

Applied EFs may polarize endothelial sprouts by promoting cathode-directed water flow through the interstitial space<sup>(9, 12, 21)</sup>. Pressure-driven flow velocity <1  $\mu$ m/s is sufficient to polarize sprout initiation and growth through collagen and fibrin gels antiparallel to the flow direction<sup>(22, 23)</sup>. We measured an average electro-osmotic mobility (EOM) of 4.2  $\pm$  0.3 nm/s/V/m through the negatively charged, porous fibrin gels in these experiments, leading to flow velocities of 0.2, 0.7, and 1.5  $\mu$ m/s in applied EFs of 50, 155, and 360 mV/mm, respectively.

The initial experiments used for studying polarization of sprouts were performed in 'open' channels, Fig. 1a, to enable media exchange. The arrangement enabled unidirectional electroosmotic flow (EOF) of media through the culture channels<sup>(11, 12)</sup>. To mimic endogenous conditions, sprouts were also exposed to EFs in 'closed' channels, Fig. 1b, where fluid pressure gradients would dissipate via backflow through the center of the low resistance fibrin pores, resulting in zero net fluid flow through the channel, Fig. 7.

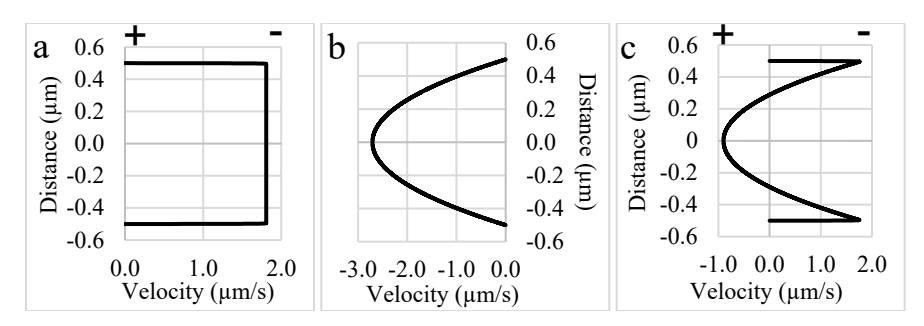


Figure 7. Cathode-directed electro-osmotic flow continues near negatively charged surfaces during zero net fluid flow in a closed channel. a. Electro-osmotic flow toward the cathode is modelled through a 1  $\mu$ m tall channel forming a plug flow profile<sup>(24)</sup>. b. A reverse direction pressure gradient is modelled and generates a parabolic flow profile through the 1  $\mu$ m tall channel with the same average volumetric flow rate. c. Simultaneous application of both flows generates slightly reduced flow velocity next to the charged walls, and backflow through the lowest resistance pathway, the center of the channel. *In vitro*, fibrin gels have pores sizes ranging from 3-10  $\mu$ m depending on preparation conditions <sup>(25, 26)</sup>. Therefore, EOF next to charged fibrin and charged sprout surfaces continues in a closed system and the pressure gradients dissipate through the low resistance center of the pores.

In the closed channels, cathode-directed EOF continues against negatively charged surfaces<sup>(27)</sup> including fibrin extracellular matrix and endothelial cell membranes, i.e. we predict that the EOM at the surface of endothelial cells is 0.7 nm/s/V/m based on the zeta potential of endothelial cells<sup>(28)</sup>. Under the conditions of no net fluid flow, sprout initiation, growth, and turning are polarized toward the anode, Fig. 5e1-e4 and Fig. 6, and there is no significant change in the number of primary sprouts, Table 1 (p > 0.5 two-tailed t-test).

In the absence of net fluid flow in the closed channels, relative sprout length facing the anode, Fig. 5e3, is significantly longer than in the same region exposed to unidirectional flow in the open channels, Fig. 5d3, 240-300° (p < 0.005) or 210-330° (p < 0.02). No significant difference exists in relative sprout length between these two conditions in the regions facing the cathode between  $60-120^{\circ}$  (p > 0.5) or  $30-150^{\circ}$  (p > 0.5). Also, no significant anodal turning occurs in closed channels on the anode side between  $180-360^{\circ}$ , Fig. 5e4. These results support a role for fluid flow during reduction of anodal growth length and during anodal turning. They also support the hypothesis that application of DC EFs *in vivo* could polarize sprout initiation and growth in porous spaces beneath the skin.

## **Asymmetric Pulsed EFs Polarize Sprouts**

To explore asymmetries in response time between polarized anodal growth and growth inhibition toward the cathode, EFs of 360 mV/mm were alternated each minute, creating a time-averaged EF of zero. Under these conditions, sprouts are not polarized, Fig. 8a1. There is no significant polarization of sprout initiation between the two poles, Fig. 6, or even between the more restricted regions where sprout initiation is parallel to the EFs between 60-120° and 240-300° (p>0.1, two-tailed t-test). There is no significant difference in the number of primary sprouts in the absence of EFs or presence of alternating EFs, Table 1 (p > 0.1). No consistent differences were

identified for sprout distribution in the regions encompassing  $60-120^{\circ}$  or  $240-300^{\circ}$ , Fig. 8a2, (p>0.1) but the average sprout length was significantly reduced to  $0.86 \pm 0.07$  of sprouts not exposed to EFs, Fig. 8a3 (p < 0.001). No significant turning was identified compared to sprouts grown in the absence of EFs, Fig. 8a4.

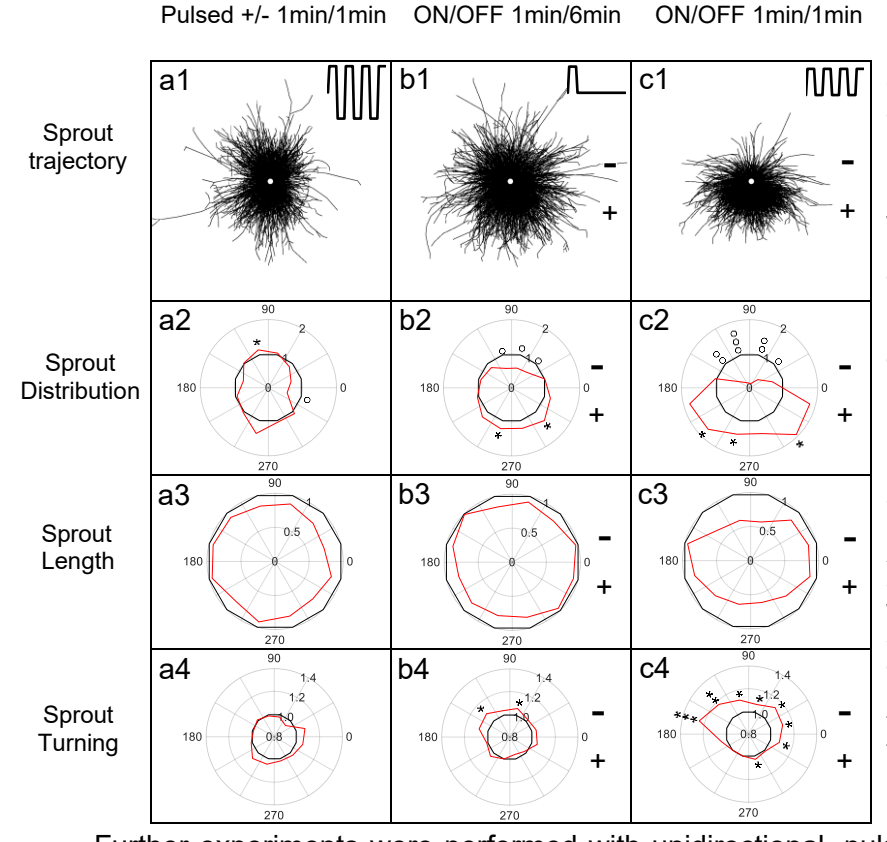


Figure 8. Sprout polarization is dependent on timethe averaged field strength. a1-c1. Unidirectional pulsed **EFs** sprout polarization. increase Insets show the applied electrical waveforms beginning at 0 mV/mm. a2-c2. Relative sprout distribution exposed to pulsed compared to the EFs (red) normalized sprout distribution determined in the absence of EFs (black). a3-c3. Relative length of sprouts exposed to pulsed EFs (red) compared to normalized sprout length in the absence of EFs (black). a4-c4. Sprout turning toward the anode,  $\Delta\cos\theta$  >1. increases with timeaveraged EF. One-tailed t-tests were used to assess statistical significance for increased (\*) or decreased (°) growth or turning. (one symbol, 0.002 ,two symbols, 0.0002 < p < 0.002, three symbols, p < 0.0002)

Further experiments were performed with unidirectional, pulsed EFs using 360 mV/mm with duty cycles of 14.3% and 50%, leading to time-averaged EFs of 51.4 and 180 mV/mm, respectively, Fig 8b1-c1. Under these conditions sprout initiation, Fig. 6, and growth, Fig 8b2-c2, are significantly polarized to the anode. There was no significant difference between the number of primary sprouts in the absence of EFs or presence of the pulsed EFs at 14.3% duty cycle or 50% duty cycle, Table 1 (p > 0.1, and p > 0.5, respectively). Relative sprout length in the presence of pulsed EFs (14.3% duty cycle) Fig. 8b3,  $0.89 \pm 0.06$ , is significantly greater than the relative sprout length in DC EFs of 50 mV/mm,  $0.75 \pm 0.5$  (p <  $10^{-5}$ , one-tailed t-test). Significant anodal turning also occurs at two cathode facing regions under these pulsed conditions, Fig. 8b4. Sprouts exposed to 360 mV/mm (50% duty cycle) have an average sprout length of  $0.76 \pm 0.13$  of control sprouts, Fig. 8c3. The average relative sprout length parallel to the EFs,  $0.62 \pm 0.06$ , is significantly shorter than the average relative length perpendicular to the EFs,  $0.90 \pm 0.08$  (p<10-8). Significant anodal turning occurs for all cathode-initiating sprouts and for two regions of the

anode-initiating sprouts, Fig. 8c4. Unidirectional pulsed EFs appear just as efficient at polarizing sprout growth as DC EFs but enable growth of longer sprouts.

### **Discussion**

Electrical therapies consisting of DC and pulsed EFs accelerate healing of chronic epidermal wounds and promote skin transplantation<sup>(29-32)</sup>. They are thought to work by mimicking or enhancing the native electric fields that occur near the wounded epidermis (100-200 mV/mm), and are capable of polarizing cell migration and growth<sup>(6, 33)</sup>. These injury-induced EFs expose local cells and extracellular matrix to a polarizing cue until the epidermal barrier and electrical resistance reform.

We provide the first evidence that EFs of similar magnitude as those near epidermal wounds, direct HUVEC migration toward the cathode, Figs. 2 & 3, and polarize endothelial sprout initiation, growth, and turning toward the anode Figs. 4-6 & 8. Sprout growth, like endothelial cell migration, appears to be dependent on guidance by one cell. The sprout tip cell is hypothesized to migrate and pull on the basal stalk cells prompting them to proliferate and increase the length of the sprout behind the tip cell<sup>(34)</sup>.

We hypothesize that electrically driven water flow, electro-osmosis, promotes sprout polarization similar to pressure driven flow<sup>(22, 23, 35)</sup>. Sprout growth in extracellular matrices is antiparallel to pressure-driven perfusion and antiparallel to electrokinetic perfusion. Pressure-driven flow velocities of only 0.3-1.0  $\mu$ m/s polarize sprout initiation and growth<sup>(22, 23)</sup> and are similar to the electro-osmotic flow velocities, 0.2 - 1.5  $\mu$ m/s, identified in these experiments. *In vitro*, low flow velocities induced by pressure-driven flow eliminate extracellular morphogen gradients and still polarize sprouts antiparallel to flow, supporting mechanotransduction as the polarizing mechanism in response to flow<sup>(35)</sup>.

Unidirectional EFs stimulate anodal initiation and inhibit cathodal initiation, Fig. 6, leading to 0.9-, 2.3- and 4.1-fold greater anodal initiation for 50, 155 and 360 mV/mm, respectively, and 0.8 and 4.0 fold greater anodal initiation for pulsed EFs with 51.4 mV/mm and 180 mV/mm time-averaged EFs. Pulsed EFs at 51.4 mV/mm were just as effective in polarizing sprout initiation as DC EFs with 50 mV/mm, (p > 0.5), and pulsed EFs at 180 mV/mm were just as effective as DC EFs at 360 mV/mm, (p > 0.5).

The electro-osmotic flow surrounding the sprouts is sufficient to polarize sprout initiation and growth in the absence of net flow through the fibrin matrix, Fig. 5e1-e4. In closed channels, sprout initiation was still polarized to the anode to the same extent as sprout initiation in open channels, Fig. 6. We conclude that net fluid flow through the fibrin is not required to polarize sprout initiation.

Applied EFs induce endothelial sprouts to turn and grow toward the anode similar to trajectory plots for some migrating cells<sup>(36)</sup> and growing spinal neurites<sup>(6)</sup>. Endothelial sprout turning was more common with higher magnitude EFs, Figs. 5b4-d4 & 8b4-c4, but was significantly altered in the absence of net fluid flow, Fig. 5e4, indicating that unidirectional fluid flow was, in part, causing the sprouts to turn into the direction of flow.

EFs significantly reduced average sprout length, compared to sprouts grown in the absence of EFs, Figs. 5b3-e3 & 8a3-c3. DC EFs of 360 mV/mm had the greatest effect in reducing average sprout length. However, the DC EFs of 50 mV/mm had greater effect in reducing sprout length than the 360 mV/mm pulsed EFs with 14.3% duty cycle that produced a time-averaged EF of 51.4 mV/mm. This indicates that the pulsed EFs are just as efficient at polarizing sprout growth but also promote growth of longer sprouts. Consistent with this hypothesis, sprout growth toward the anode is significantly more impaired parallel to the EF vector compared to sprout growth perpendicular to the EF vector.

Shorter anode growing sprouts may be a result of having to grow against fluid flow. The average length of sprouts exposed to alternating EFs was reduced to 86% of the average sprout length in the absence of EFs. There would have been no net movement of extracellular growth factors in alternating EFs, however alternating fluid flow would be present at a rate of 1.5 µm/s through the fibrin matrix. Also consistent with this hypothesis, sprouts grown in a DC EF of 360 mV/mm in the absence of net fluid flow, Fig. 5e3, grew significantly longer in the region facing the anode 210-330° than sprouts exposed to the same EF strength in the open channels exposed to unidirectional fluid flow toward the cathode Fig. 5d3. While EFs promoted sprout polarization toward the anode and antiparallel to EOF, the flow rate appears to have impeded anodal growth length especially at the higher DC EFs.

We hypothesize that the changes in electrical polarity between migrating endothelial cells and growing endothelial sprouts help to promote revascularization during wound healing. The native electrical polarity of the epidermal wound bed<sup>(6)</sup> could promote vasculogenesis by directing single endothelial precursors or endothelial cells toward the center of the wound (cathode), Fig. 9 (top). Endothelial sprouts that form in the wound bed after vasculogenesis will be directed back toward the edge of the wound (anode) where they can anastomose with the existing vasculature. Under pathological conditions in chronic wounds, that appear to stall in the inflammatory phase of healing <sup>(30)</sup>, applied EFs may promote EOF in the interstitial space. Enhanced interstitial flow may flush inflammatory mediators out of the wound bed while enhancing access to nutrients necessary for the proliferation and remodeling phases of wound healing <sup>(11, 12)</sup>. In addition applied

EFs may amplify and extend the native EFs and EOF further away from the wound site to promote revascularization of the wound which is necessary for healing (30).

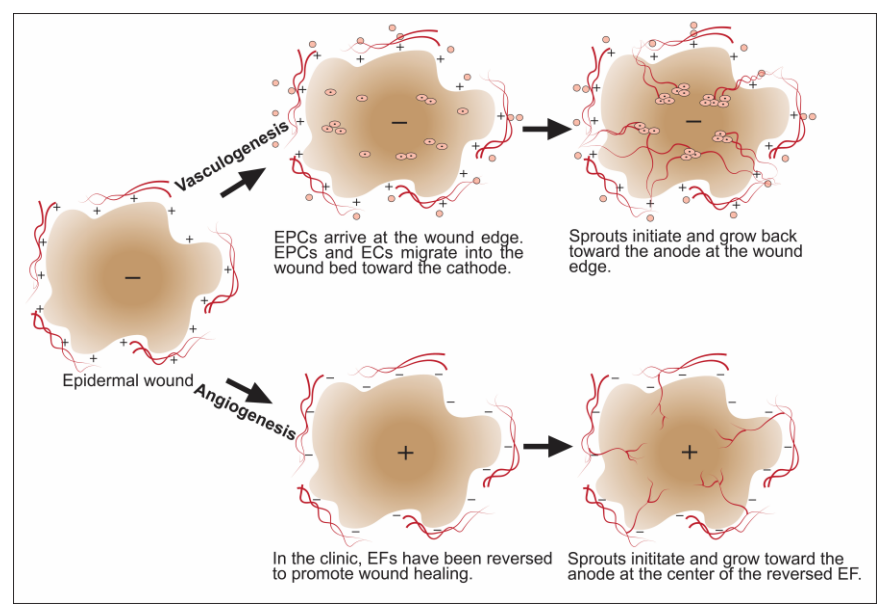


Figure 9. Models describing electrical sprout polarization during normal wound healing (top) and when therapeutic applied EFs are reversed (TOP) Endothelial (bottom). precursor cells (EPCs) and endothelial cells (ECs) migrate toward the cathode in applied EFs, and are predicted to migrate to the center of a wound based on the native electrical polarity. Initiation and growth of endothelial sprouts originating from the EPCs and ECs near the center of the wound bed will be directed back toward the edge of the wound, the electrical anode. (BOTTOM) Reversal of the native wound EF has also been found to increase

the rate of healing of chronic epidermal wounds. Under these conditions, sprouts at the edge of the wound would initiate and grow toward the center of the wound, promoting vascularization of the wound bed.

Reversal of the electrical polarity of epidermal wounds, by placing the anode electrode on the wound bed, is also reported to promote wound healing<sup>(29, 37)</sup>, Fig. 9 (bottom). Under these conditions, EFs could promote angiogenesis and sprout growth into the wound bed from vessels surrounding the wound. The reversed EFs may be especially necessary to help treat chronic wounds that are associated with poor or damaged vasculature or skin transplants that require vascularization to promote survival.

Electro-osmotic flow has significant advantages over pressure-driven flow in constrained spaces in tissues. EOF makes use of the native negative charge of extracellular matrices and cell surfaces to promote relatively uniform flow velocity between pores of different dimensions<sup>(11, 12)</sup> while pressure-driven flow is impeded by both the local charge<sup>(38)</sup> and pore size dependent drag according to Poiseuille. As a result, pressure-driven flow causes tissue compaction and increases hydraulic resistance<sup>(39, 40)</sup>. EOF can be induced across skin due to electroporation<sup>(41)</sup> and the flow path can be predicted between two electrical poles based on electrical resistance in the extracellular space. We hypothesize that EFs applied to promote healing of chronic epidermal wounds and transplantation of skin can influence polarization and growth of endothelial sprouts into the wound bed *in vivo* and may be a critical factor to promote healing. EFs may also be useful to reduce or prevent neovascularization of tissues such as in the cornea that can lead to blindness<sup>(42)</sup>.

### References

- 1. Lovett M, Lee K, Edwards A, & Kaplan DL (2009) Vascularization strategies for tissue engineering. *Tissue Engineering Part B, Reviews* 15(3):353-370.
- 2. Novosel EC, Kleinhans C, & Kluger PJ (2011) Vascularization is the key challenge in tissue engineering. *Advanced Drug Delivery Reviews* 63:300-311.
- 3. Xu K & Cleaver O (2011) Tubulogenesis during blood vessel formation. *Semin. Cell Dev. Biol.* 22(9):993-1004.
- 4. Lamalice L, Le Boeuf F, & Huot J (2007) Endothelial cell migration during angiogenesis. *Circulation Research* 100:782-794.
- 5. Vavourakis V, Wijeratne PA, Shipley R, Loizidou M, Stylianopoulos T, & Hawkes DJ (2017) A validated multiscale in-silico model for mechano-sensitive tumour angiogenesis and growth. *PLOS Computation Biology* 13(1):e1005259.
- 6. McCaig CD, Rajnicek AM, Song B, & Zhao M (2005) Controlling cell behavior electrically: Current views and future potential. *Physiological Reviews* 85:943-978.
- 7. Messerli MA & Graham DM (2011) Extracellular electrical fields direct wound healing and regeneration. *Biological Bulletin* 221:79-92.
- 8. Nuccitelli R (2004) A role for endogenous electric fields in wound healing. *Current Topics in Developmental Biology*, ed Schatten ED (Academic Press, San Diego, CA), Vol 58, pp 1-26.
- 9. Sarkar A, Kobylkevich BM, Graham DM, & Messerli MA (2019) Electromigration of cell surface macromolecules in DC electric fields during cell polarization and galvanotaxis. *Journal of Theoretical Biology* 478:58-73.
- 10. Allen GM, Mogilner A, & Theriot JA (2013) Electrophoresis of cellular membrane components creates the directional cue guiding keratocyte galvanotaxis. *Current Biology* 23:560-568.
- 11. Sarkar A & Messerli MA (2021) Electrokinetic perfusion through three-dimensional culture reduces cell mortality. *Tissue Engineering Part A* 27(23-24):1470-1479.
- 12. Walker JC, Jorgensen AM, Sarkar A, Gent SP, & Messerli MA (2022) Anionic polymers amplify electrokinetic perfusion through extracellular matrices. *Frontiers in Bioengineering and Biotechnology*:1786.
- 13. Long H, Yang G, & Wang Z (2011) Galvanotactic migration of EA.Hy926 endothelial cells in a novel designed electric field bioreactor. *Cell Biochemistry and Biophysics* 61(3):481-491.
- 14. Zhao Z, Qin L, Reid B, Pu J, Hara T, & Zhao M (2012) Directing migration of endothelial progenitor cells with applied DC electric fields. *Stem Cell Research* 8:38-48.
- 15. Mishra S & Vazquez M (2017) A Gal-MµS device to evaluate cell migratory response to combined galvano-chemotactic fields. *Biosensors* 7(4):54.
- 16. Ud-Din S, Sebastian A, Giddings P, Colthurst J, Whiteside S, Morris J, Nuccitelli R, Pullar C, Baguneid M, & Bayat A (2015) Angiogenesis is induced and wound size is reduced by electrical stimulation in an acute wound healing model in human skin. *PLOS One* 10(4):e0124502.
- 17. Kanno S, Oda N, Abe M, Saito S, Hori K, Handa Y, Tabayashi K, & Sato Y (1999) Establishment of a simple and practical procedure applicable to therapeutic angiogenesis. *Circulation* 99:2682-2687.
- 18. Nakatsu MN & Hughes CCW (2008) An optimized three-dimensional *in vitro* model for the analysis of angiogenesis. *Methods in Enzymology* 443:65-82.
- 19. Heiss M, Hellström M, Kalén M, May T, Weber H, Hecker M, Augustin HG, & Korff T (2015) Endothelial cell spheroids as a versatile tool to study angiogenesis *in vitro*. *FASEB Journal* 29(7):3076-3084.

- 20. Newman AC, Nakatsu MN, Chou W, Gershon PD, & Hughes CCW (2011) The requirement for fibroblasts in angiogenesis: fibroblast-derived matrix proteins are essential for endothelial cell lumen formation. *Molecular Biology of the Cell* 22(20):3791-3800.
- 21. Kobylkevich BM, Sarkar A, Carlberg BR, Huang L, Ranjit S, Graham DM, & Messerli MA (2018) Reversing the direction of galvanotaxis with controlled increases in boundary layer viscosity. *Physical biology* 15(3):036005.
- 22. Kim S, Chung M, Ahn J, Lee S, & Jeon NL (2016) Interstitial flow regulates angiogenic response and phenotype of endothelial cells in a 3D culture model. *Lab on a Chip* 16(21):4189-4199.
- 23. Abe Y, Watanabe M, Chung S, Kamm RD, Tanishita K, & Sudo R (2019) Balance of interstital flow magnitude and vascular endothelial growth factor concentration modulates three-dimensional microvascular network formation. *APL Bioengineering* 3(3):036102.
- 24. Soderman O & Jonsson B (1996) Electro-osmosis: Velocity profiles in different geometries with both temporal and spatial resolution. *Journal of Chemical Physics* 105(23):10300-10311.
- 25. Mooney R, Tawil B, & Mahoney M (2010) Specific fibrinogen and thrombin concentrations promote neuronal rather than glial growth when primary neural cells are seeded within plasma-derived fibrin gels. *Tissue Engineering: Part A* 16(5):1607-1619.
- 26. Chiu CL, Hecht V, Duong H, Wu B, & Tawil B (2012) Permeability of three-dimensional fibrin constructs corresponds to fibrinogen and thrombin concentrations. *Bioresearch open access* 1(1):34-40.
- 27. Ooi KT, Yang C, Chai JC, & Wong TN (2005) Developing electro-osmotic flow in closed-end micro-channels. *International Journal of Engineering Science* 43(17-18):1349-1362.
- 28. Ribeiro MMB, Domingues MM, Freire JM, Santos NC, & Castanho MARB (2012) Translocating the blood-brain barrier using electrostatics. *Frontiers in Cellular Neuroscience* 6:44.
- 29. Kloth LC & Zhao M (2010) Endogenous and exogenous electrical fields for wound healing. *Wound healing: Evidence-based management*, eds McCulloch JM & Kloth LC (F.A. Davis, Philadelphia), pp 450-513.
- 30. Frykberg RG & Banks J (2015) Challenges in the treatment of chronic wounds. *Advances in Wound Care* 4(9):560-582.
- 31. Souza AK, Souza TR, das Neves LMS, Leite GDPMF, Garcia SB, de Jesus Guirro RR, Barbosa RI, & de Oliveira Guirro EC (2019) Effect of high voltage pulsed current on the integration of total skin grafts in rats submitted to nicotine action. *Journal of Tissue Viability* 28(3):161-166.
- 32. Mehmandoust FG, Torkaman G, Firoozabadi M, & Talebi G (2007) Anodal and cathodal pulsed electrical stimulation on skin wound healing in guinea pigs. *Journal of Rehabilitation and Development* 44(4):611.
- 33. Isseroff RR & Dahle SE (2012) Electrical stimulation therapy and wound healing: Where are we now? *Advances in Wound Care* 1:238-243.
- 34. De Smet F, Segura I, De Bock K, Hohensinner PJ, & Carmeliet P (2009) Mechanisms of vessel branching, filopodia on endothelial tip cells lead the way. *Arteriosclerosis, thrombosis, and vascular biology* 29(5):639-649.
- 35. Shirure VS, Lezia A, Tao A, Alonzo LF, & George SC (2017) Low levels of physiological interstitial flow eliminate morphogen gradients and guide angiogenesis. *Angiogenesis* 20:493-504.
- 36. Huang L, Cormie P, Messerli MA, & Robinson KR (2009) The involvement of Ca<sup>2+</sup> and integrins in directional repsonses of zebrafish keratocytes to electric fields. *Journal of Cellular Physiology* 219:162-172.
- 37. Polak A, Franek A, & Taradaj J (2014) High-voltage pulsed current electrical stimulation in wound treatment. *Advances in Wound Care* 3(2):104-117.

- 38. Mattern KJ, Nakornchai C, & Deen WM (2008) Darcy permeability of agarose-glycosaminoglycan gels analyzed using fiber-mixture and donnan models. *Biophysical Journal* 95:648-656.
- 39. Shi Z-D, Ji X-Y, Qazi H, & Tarbell JM (2009) Interstital flow promotes vascular fibroblast, myofibroblast, and smooth muscle cell motility in 3-D collagen I via upregulation of MMP-1. *American Journal of Physiology-Heart and Circulatory Physiology* 297(4):H1225-H1234.
- 40. McCarty WJ & Johnson M (2007) The hydraulic conductivity of Matrigel<sup>™</sup>. *Biorheology* 44(5-6):303-317.
- 41. Chizmadzhev YA, Indenbom AV, Kuzmin PI, Galichenko SV, Weaver JC, & Potts RO (1998) Electrical properties of skin at moderate voltages: contribution of appendageal macropores. *Biophysical Journal* 74:843-856.
- 42. Gupta D & Illingworth C (2011) Treatments for corneal neovascularization: A review. *Cornea* 30(8):927-938.

# Acknowledgements

This research was funded by NSF award #2033522 to MM.

### **Conflict of Interest**

The authors have no relevant financial or non-financial conflicts of interest to disclose.

### **Ethics Statement**

The authors confirm that the ethical policies of the journal, as noted on the journal's author guidelines page, have been adhered to.